

Solitonic dispersive hydrodynamics: theory and observation

Michelle D. Maiden,¹ Dalton V. Anderson,¹ Nevil A. Franco,¹ Gennady A. El,² and Mark A. Hoefer^{1,*}

¹*Department of Applied Mathematics, University of Colorado, Boulder, Colorado 80309-0526, USA*

²*Department of Mathematical Sciences, Loughborough University, Loughborough, LE11 3TU, UK*

(Dated: April 6, 2024)

Ubiquitous nonlinear waves in dispersive media include localized solitons and extended hydrodynamic states such as dispersive shock waves. Despite their physical prominence and the development of thorough theoretical and experimental investigations of each separately, experiments and a unified theory of solitons and dispersive hydrodynamics are lacking. Here, a general soliton-mean field theory is introduced and used to describe the propagation of solitons in macroscopic hydrodynamic flows. Two universal adiabatic invariants of motion are identified that predict trapping or transmission of solitons by hydrodynamic states. The result of solitons incident upon smooth expansion waves or compressive, rapidly oscillating dispersive shock waves is the same, an effect termed hydrodynamic reciprocity. Experiments on viscous fluid conduits quantitatively confirm the soliton-mean field theory with broader implications for nonlinear optics, superfluids, geophysical fluids, and other dispersive hydrodynamic media.

Long wavelength, hydrodynamic theories abound in physics, from fluids [1] to optics [2], condensed matter [3] to quantum mechanics [4], and beyond. Such theories describe expansion and compression waves until breaking. When the physics at shorter wavelengths are predominantly dispersive, dispersive hydrodynamic theories [5, 6] are used to describe shock waves of a spectacularly different character than their dissipative counterparts. Dispersive shock waves (DSWs) consist of coherent, rank-ordered, nonlinear oscillations that continually expand [6, 7]. Observations in a wide range of physical media that include quantum matter [8, 9], optics [10, 11], classical fluids [12, 13] and magnetic materials [14] demonstrate the prevalence of DSWs.

Another celebrated feature of dispersive hydrodynamic media are localized, nonlinear solitary waves. When they exhibit particle-like properties such as elastic, pairwise interactions, solitary waves are called solitons [15] and have been extensively studied both theoretically [16] and experimentally [17]. The focus here is on solitary waves that exhibit solitonic behavior, i.e., elastic or near-elastic interaction, henceforth we refer to them as solitons. Despite their common origins, solitons and dispersive hydrodynamics have been primarily studied independently.

Utilizing the scale separation between extended hydrodynamic states and localized solitons (see Fig. 1), we propose in this work a general theory of solitonic dispersive hydrodynamics encapsulated by a set of effective partial differential equations for the hydrodynamic mean field, the soliton's amplitude, and its phase. We identify two adiabatic invariants of motion and show that they lead to two pivotal predictions. First, the soliton trajectory is a characteristic of the governing equations that is directed by the mean field, a nonlinear analogue of wavepacket trajectories in quantum mechanics [4]. This implies that solitons are either trapped by or transmitted through a hydrodynamic state, depending on the relative amplitudes of the soliton and the hydrodynamic “barrier”.

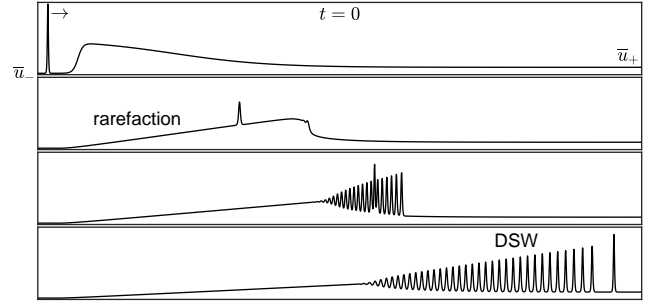


FIG. 1. Representative initial configuration and evolution (top to bottom) for solitonic dispersive hydrodynamics. The narrow soliton on the uniform mean field \bar{u}_- is transmitted through the broad hydrodynamic flow if it reaches and propagates freely on the uniform mean field \bar{u}_+ . The hydrodynamic flow exhibits expansion (rarefaction) and compression that leads to a dispersive shock wave.

The second prediction we term hydrodynamic reciprocity. Given an incident soliton amplitude and the far-field mean conditions, the adiabatic invariants are used to predict when the soliton is trapped or transmitted and, in the latter case, what its transmitted amplitude and phase shift are. Hydrodynamic reciprocity means that the trapping, transmission amplitude/phase relations are the same for soliton interactions with smooth, expanding rarefaction waves (RWs) and compressive, oscillatory DSWs.

We confirm these predictions with experiments on the interfacial dynamics of a viscous fluid conduit, a model dispersive hydrodynamic medium [18] that has been used previously to investigate solitons [19–21] and DSWs [13]. Although soliton-DSW interaction has been observed previously [13], the nature and properties of the interaction were not explained. We stress that the theory presented is general and applies to a wide range of physical media [8–14].

Experiments are performed on the interfacial dynam-

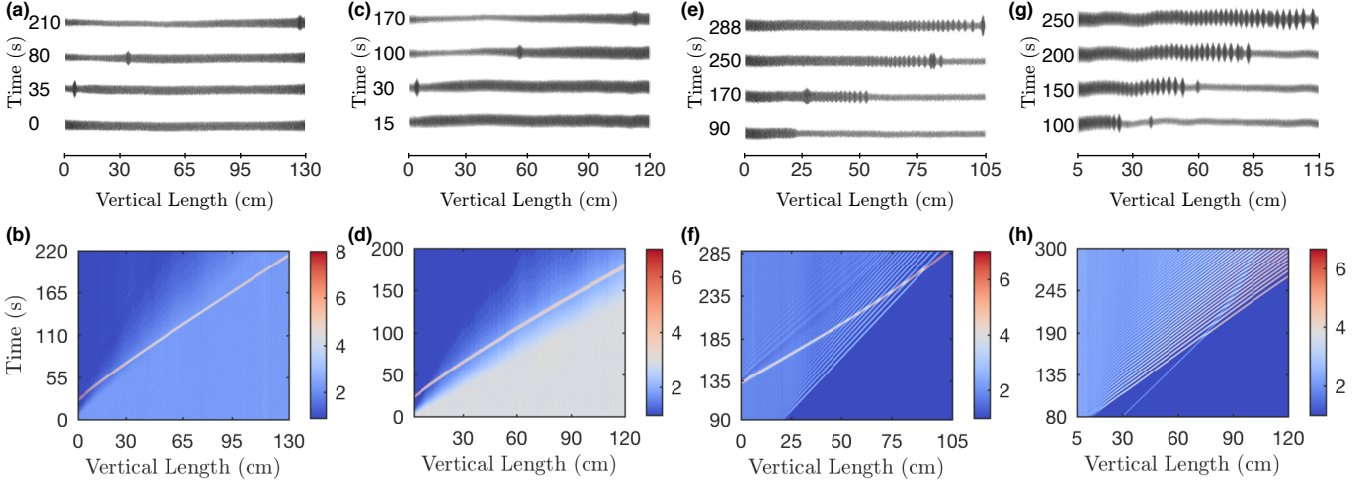


FIG. 2. Experiments demonstrating soliton transmission and trapping with hydrodynamic states. Representative image sequences (a,c,e,g) and space-time contours (b,d,f,h) extracted from image processing are shown. The contour intensity scale is the dimensionless conduit cross-sectional area relative to the smallest area. a,b) Soliton-RW transmission. c,d) Soliton-RW trapping. e,f) Soliton-DSW transmission. g,h) Soliton-DSW trapping.

ics of a buoyant, viscous fluid injected from below into a miscible, much more viscous fluid matrix. Due to negligible diffusion and high viscosity contrast, the two-fluid interface serves as the dispersive hydrodynamic medium [18, 19]. The experimental setup is similar to that described in [13] and consists of a tall acrylic column filled with glycerol (viscosity 1.2 ± 0.2 P, density 1.2587 ± 0.0001 g/cm³). A nozzle at the column base serves as the injection point for the interior fluid (viscosity 0.51 ± 0.01 P, density 1.2286 ± 0.0001 g/cm³), a miscible solution of glycerol, water, and black food coloring. By injecting at a constant rate (0.25 mL/min or 0.77 mL/min), the buoyant interior fluid establishes a vertically uniform fluid conduit. Although predicted to be unstable, our experiment operates in the convective regime [22]. By varying the injection rate, conduit solitons, RWs, and DSWs can be generated at the interface between the interior and exterior fluids.

Observations of the hydrodynamic transmission and trapping of solitons resulting from their interaction with RWs and DSWs are depicted in Fig. 2. The contour plots in 2(b,f) show that transmitted solitons exhibit a smaller (larger) amplitude and faster (slower) speed post interaction with a RW (DSW). The transmitted solitons experience a phase shift due to hydrodynamic interaction, defined as the difference between the post and pre interaction spatial intercept. Our measurements show a negative (positive) phase shift for the soliton transmitted through a RW (DSW). Sufficiently small incident solitons in Fig. 2(d,h) do not emerge from the RW or DSW interior during the course of experiment, remaining trapped inside the hydrodynamic state.

We now present a theory to explain these observations by considering a general dispersive hydrodynamic

medium with nondimensional scalar quantity $u(x, t)$ (e.g., conduit cross-sectional area) governed by

$$u_t + V(u)u_x = D[u]_x, \quad x \in \mathbb{R}, \quad t > 0. \quad (1)$$

$V(u)$ is the long-wave speed, $D[u]$ is an integro-differential operator, and Eq. (1) admits a real-valued, linear dispersion relation with frequency $\omega(k, \bar{u})$ where k is the wavenumber and \bar{u} is the background mean field. We assume $V'(u) > 0$ so that the dispersive hydrodynamic system has convex flux [23]. The dispersion is assumed negative ($\omega_{kk} < 0$) for definiteness. We also assume that equation (1) satisfies the prerequisites for Whitham theory, an approximate description of modulated nonlinear waves that accurately characterizes dispersive hydrodynamics in a wide-range of physical systems [5, 6].

Many models can be expressed in the form (1). In the Appendix, we perform calculations for the Korteweg-de Vries (KdV) equation $V(u) = u$, $D[u] = -u_{xx}$, a universal model of weakly nonlinear, dispersive waves, and the conduit equation $V(u) = 2u$, $D[u] = u^2(u^{-1}u_t)_x$, an accurate model for our experiments [18].

The dynamics of DSWs, RWs, and solitons for Eq. (1) can be described using Whitham theory [5], where a nonlinear periodic wave's mean \bar{u} , amplitude a , and wavenumber k are assumed to vary slowly via modulation equations. The modulation equations admit an asymptotic reduction in the non-interacting soliton wavetrain regime $0 < k \ll 1$ [24, 25]

$$\begin{aligned} \bar{u}_t + V(\bar{u})\bar{u}_x &= 0, & a_t + c(a, \bar{u})a_x + f(a, \bar{u})\bar{u}_x &= 0, \\ k_t + [c(a, \bar{u})k]_x &= 0. \end{aligned} \quad (2)$$

The first equation is for the decoupled mean field, which is governed by the dispersionless, $D \rightarrow 0$, equation (1).

The second equation describes the soliton amplitude a , which is advected by the mean field according to the soliton amplitude-speed relation $c(a, \bar{u})$ and the coupling function $f(a, \bar{u})$. The final equation expresses wave conservation [5] and describes a train of solitons with spacing $2\pi/k \gg 1$. The soliton train here is a useful, yet fictitious construct because we will only consider the soliton limit $k \rightarrow 0$ of solutions to Eq. (2). Equation (2) with $c(a, \bar{u}) = a/3 + \bar{u}$ and $f(a, \bar{u}) = 2a/3$ corresponds to the soliton limit of the KdV-Whitham system of modulation equations, shown in [26] to be equivalent to the soliton modulation equations determined by other means [24] with application to shallow water soliton propagation over topography in [24, 27–29]. The general case of Eq. (2) was derived in [25] and can be interpreted as a mean field approximation for the interaction of a soliton with the hydrodynamic flow. In contrast to standard soliton perturbation theory where the soliton's parameters evolve temporally [30], solitonic dispersive hydrodynamics require the soliton amplitude $a(x, t)$ be treated as a spatio-temporal field. We note that the equations in (2) can be solved sequentially by the method of characteristics [24].

It will be physically revealing to diagonalize the system of equations in (2) by identifying its Riemann invariants [5]. Owing to the special structure of (2) with just two characteristic velocities $V < c$, it is always possible to find a change of variables to Riemann invariant form that diagonalizes the system. The mean field equation is already diagonalized with \bar{u} the Riemann invariant associated to the velocity V . The second Riemann invariant, $q = q(a, \bar{u})$ is associated with the velocity c . q can be found by integrating the differential form $f d\bar{u} + (c - V) da$ [5] (see the Appendix). For KdV, $q(a, \bar{u}) = a/2 + \bar{u}$, whereas for the conduit equation

$$\begin{aligned} c(a, \bar{u}) &= [\bar{u}^2 + (a + \bar{u})^2(2 \ln(1 + a/\bar{u}) - 1)]\bar{u}/a^2, \\ q(a, \bar{u}) &= c(a, \bar{u})[c(a, \bar{u}) + 2\bar{u}]/\bar{u}. \end{aligned} \quad (3)$$

The third Riemann invariant is found by direct integration of the wavenumber equation to be the quantity $kp(q, \bar{u})$ given by

$$p(q, \bar{u}) = \exp \left(- \int_{\bar{u}_0}^{\bar{u}} \frac{C_u(q, u)}{V(u) - C(q, u)} du \right), \quad (4)$$

where $C(q(a, \bar{u}), \bar{u}) \equiv c(a, \bar{u})$. For KdV, $p(q, \bar{u}) = (q - \bar{u})^{-1/2}$. The change of variables $q = q(a, \bar{u})$ and $p = p(q, \bar{u})$ diagonalizes (2)

$$\begin{aligned} \bar{u}_t + V(\bar{u})\bar{u}_x &= 0, & q_t + C(q, \bar{u})q_x &= 0, \\ (kp)_t + C(q, \bar{u})(kp)_x &= 0. \end{aligned} \quad (5)$$

We seek solutions to Eq. (5) subject to an initial mean field profile $\bar{u}(x, 0) = \bar{u}_0(x)$ and an initial soliton of amplitude a_0 located at $x = x_0$. But we require initial soliton and wavenumber fields $a(x, 0)$ and $k(x, 0)$ for all x in

order to give a properly posed problem for (2). Admissible initial conditions are obtained by recognizing this as a special solution, a simple wave in which all but one of the Riemann invariants are constant [5]. The non-constant Riemann invariant must be \bar{u} to satisfy the initial condition and therefore satisfies $\bar{u} = \bar{u}_0(x - V(\bar{u})t)$. The initial soliton amplitude and position determine the constant Riemann invariant $q_0 = q(a_0, \bar{u}_0(x_0))$. An initial wavenumber k_0 determines the other constant Riemann invariant $k_0 p_0 = k_0 p(q_0, \bar{u}_0(x_0))$. As we will show, the value of $k_0 > 0$ is not relevant so can be arbitrarily chosen. We now show how this solution physically describes soliton-mean field interaction.

A smooth, initial mean field, e.g., in Fig. 1, will evolve according to the obtained implicit solution until wave-breaking occurs. Our interest is in the interaction of a soliton with the expansion and compression waves that result. In dispersive hydrodynamics, the simplest examples of these are RWs and DSWs, respectively, which are most conveniently generated from step initial data. We therefore analyze the obtained general solution subject to step initial data

$$\bar{u}(x, 0) = \bar{u}_{\pm}, \quad a(x, 0) = a_{\pm}, \quad k(x, 0) = k_{\pm}, \quad \pm x > 0, \quad (6)$$

that model incident and transmitted soliton amplitudes a_- and a_+ through the mean field transition \bar{u}_- to \bar{u}_+ for soliton train wavenumbers k_- and k_+ . The mean field dynamics depend upon the ordering of \bar{u}_- and \bar{u}_+ . When $\bar{u}_- < \bar{u}_+$, the mean field equation admits a RW solution, otherwise an unphysical, multi-valued solution. Short-wave dispersion regularizes such behavior and leads to the generation of a DSW. We consider each case in turn.

The transmission of a soliton through a RW is shown experimentally in Fig. 2(a,b). The incident soliton “climbs” the RW and emerges from the interaction with altered amplitude and speed. The mean field is the self-similar, RW solution with $u(x, t) = \bar{u}_{\pm}$ for $\pm x > \pm V_{\pm}t$ and

$$\bar{u}(x, t) = V^{-1}(x/t), \quad V_-t \leq x \leq V_+t, \quad (7)$$

where $V_{\pm} = V(\bar{u}_{\pm})$ and V^{-1} is the inverse of V . Constant q and kp correspond to adiabatic invariants of the soliton-mean field dynamics that yield constraints on the amplitude, mean field, and wavenumber parameters we call the *transmission and phase conditions*

$$q(a_-, \bar{u}_-) = q(a_+, \bar{u}_+), \quad \frac{k_-}{k_+} = \frac{p(q_+, \bar{u}_+)}{p(q_-, \bar{u}_-)}. \quad (8)$$

The first adiabatic invariant $q(a, \bar{u})$ determines the transmitted soliton amplitude a_+ in terms of the incident soliton amplitude a_- and the mean fields \bar{u}_{\pm} . The second adiabatic invariant determines the ratio k_-/k_+ , which in turn yields the soliton's phase shift due to hydrodynamic interaction. Equation (8) is the main theoretical result

of this work and describes the trapping or transmission of a soliton through a RW and a DSW.

The necessary and sufficient condition for soliton transmission is a positive transmitted soliton amplitude $a_+ > 0$, which places a restriction on the incident soliton amplitude a_- . For the conduit equation, Eq. (3) implies $c_- > c_{cr} = -\bar{u}_- + (\bar{u}_-^2 + 8\bar{u}_+\bar{u}_-)^{1/2}$. For KdV, $a_- > a_{cr} = 2(\bar{u}_+ - \bar{u}_-)$. In both cases, we find that the transmitted soliton's amplitude is decreased, $a_+ < a_-$ and its speed is increased, $c_+ > c_-$. More generally, $\text{sgn}(a_+ - a_-) = -\text{sgn}(q\bar{u}q_a)$ and $\text{sgn}(c_+ - c_-) = \text{sgn}(C_{\bar{u}})$ (see Appendix).

The soliton phase shift is $\Delta = x_+ - x_-$ where x_{\pm} are the x -intercepts of the soliton pre (-) and post (+) hydrodynamic interaction. Given the initial soliton position x_- , the contraction/expansion of the soliton train determines the phase shift as $\Delta/x_- = k_-/k_+ - 1 = p_+/p_- - 1$. Hence, the ratio k_-/k_+ in the phase condition (8), not the arbitrary initial wavenumber k_- , determines the soliton phase shift. Our use of a fictitious soliton train is therefore justified.

We also determine the soliton-RW trajectory. A soliton with position $x(t)$ propagates through the mean field along a characteristic of the modulation system (2)

$$\frac{dx}{dt} = C(q, \bar{u}(x, t)), \quad x(0) = x_-, \quad (9)$$

where the soliton amplitude $a(x, t)$ varies along the trajectory according to the adiabatic invariant $q(a(x, t), \bar{u}(x, t)) = q(a_-, \bar{u}_-)$. The phase shift from integration of (9) equals Δ from the adiabatic invariant in (8), as expected.

When $a_+ \leq 0$ in (8), the soliton is trapped by the RW, as in experiment, Fig. 2(c,d).

If $\bar{u}_- > \bar{u}_+$, a DSW is generated. Soliton-DSW transmission is experimentally depicted in Fig. 2(e,f). An incident soliton propagates through the DSW, exhibiting a highly non-trivial interaction, ultimately emerging with altered amplitude and speed.

In contrast to the soliton-RW problem, the modulation equations (2) are no longer valid throughout the soliton-DSW interaction. Instead, the mean field equation is replaced by the DSW modulation equations [6, 7]. We seek a simple wave solution for soliton-DSW modulation. Because DSW generation occurs only for $t > 0$, the soliton-DSW modulation system for $t < 0$ reduces exactly to Eq. (2), i.e., that of soliton-RW modulation. For $t < 0$, the adiabatic invariants (8) hold. By continuity of the modulation solution, these conditions must hold for $t \geq 0$ as well. In particular, soliton-RW and soliton-DSW interaction both satisfy *the same transmission and phase conditions* (8). This fact, termed hydrodynamic reciprocity, is due to time reversibility of the governing equation (1) and is depicted graphically in Fig. 3.

Equations (3) and (8) for the conduit equation indicate that solitons incident upon DSWs exhibit a decreased

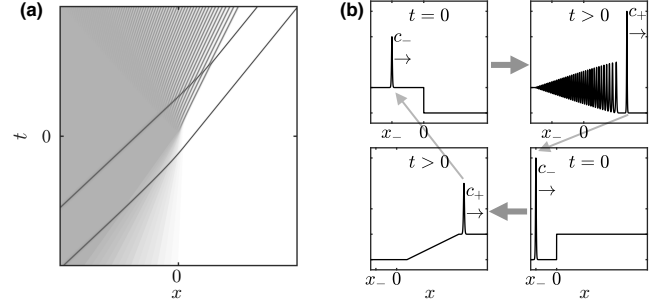


FIG. 3. Graphical depictions of hydrodynamic reciprocity. (a) Space-time contour plot of soliton-DSW ($t > 0$) and soliton-RW ($t < 0$) interaction with two solitons satisfying the transmission condition (8). For $|t|$ sufficiently large, the soliton speeds are the same. (b) If the soliton post DSW interaction (top, left to right) is used to initialize soliton-RW interaction (bottom, right to left), the post RW interaction soliton has the same properties as the pre DSW interaction soliton.

transmitted speed $c_{cr} < c_+ < c_-$ and an increased transmitted amplitude $a_+ > a_{cr} > a_-$. a_{cr} and c_{cr} are precisely the amplitude and speed of the DSW's soliton leading edge [31]. Hydrodynamic reciprocity therefore implies that the transmitted soliton's amplitude is decreased (increased), its speed is increased (decreased), and its phase shift is negative (positive) relative to the soliton incident upon the RW (DSW), as observed experimentally in Fig. 2. Using the transmission and phase conditions (8), we accurately predict the conduit soliton trajectory post DSW interaction without any detailed knowledge of soliton-DSW interaction (see Appendix).

In contrast to soliton-RW transmission, solitons with amplitude a_+ initially placed to the right of the step will interact with the DSW if $a_+ < a_{cr}$. Then the transmission condition (8) implies $a_- < 0$, i.e., the soliton cannot transmit back through the DSW. Instead, the soliton is effectively trapped as a localized defect in the DSW interior as observed experimentally in Fig. 2(g,h).

The transmission and phase conditions (8) for the conduit equation are shown in Fig. 4. For soliton-RW interaction, the abscissa and ordinate are a_- and a_+ , respectively reversed for soliton-DSW interaction. Hydrodynamic reciprocity implies that the transmission condition on these axes is the same for soliton-RW and DSW transmission. Reciprocity is confirmed by experiment and numerical simulations of the conduit equation in Fig. 4(a), that slightly deviate from soliton-mean field theory as the amplitudes increase, consistent with previously observed discrepancies [13, 31]. Reciprocity of the phase shift is also confirmed by conduit equation numerics in Fig. 4(b). Our experiments provide definitive evidence of soliton-hydrodynamic transmission, trapping, reciprocity, and the theory's efficacy.

We have introduced a general framework for soliton-

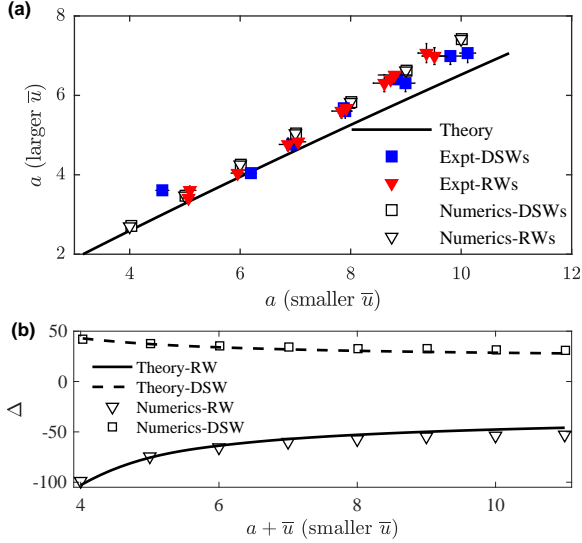


FIG. 4. Transmitted soliton properties due to conduit soliton-RW and DSW interaction for a hydrodynamic transition from $\bar{u} = 1$ to $\bar{u} = 1.75$. a) Soliton amplitude from eq. (8) (curve), experiment (filled squares, triangles), and numerical simulations (open squares, triangles). b) Soliton phase shift from eq. (8) (curves) and numerical simulations (symbols).

mean field interaction. The dynamics exhibit two adiabatic invariants that describe soliton trapping or transmission. The existence of the same adiabatic invariants for soliton-mean field interactions of compression (DSW) and expansion (RW) imply hydrodynamic reciprocity. This describes a conceptually new notion of hydrodynamic soliton “tunneling” where the potential barrier is the mean field, obeying the same equations as the soliton [32].

Appendix A: Riemann invariants of solitonic hydrodynamics

In this section, we provide the derivation of the Riemann invariants for the soliton train modulation system

$$\bar{u}_t + V(\bar{u})\bar{u}_x = 0, \quad (\text{A10a})$$

$$a_t + c(a, \bar{u})a_x + f(a, \bar{u})\bar{u}_x = 0, \quad (\text{A10b})$$

$$k_t + [c(a, \bar{u})k]_x = 0, \quad (\text{A10c})$$

enabling its reduction to the diagonal form

$$\bar{u}_t + V(\bar{u})\bar{u}_x = 0, \quad (\text{A11a})$$

$$q_t + C(q, \bar{u})q_x = 0, \quad (\text{A11b})$$

$$(kp)_t + C(q, \bar{u})(kp)_x = 0. \quad (\text{A11c})$$

To elucidate the general procedure, we perform explicit calculations for the KdV equation along with the conduit equation, our primary example.

First, we notice that equations (A10a) and (A10b) are decoupled from (A10c), and have two distinct, real characteristic velocities $V < c$. This 2×2 subsystem of quasilinear equations is thus strictly hyperbolic and can be diagonalized for any coupling function $f(a, \bar{u})$ [5].

The mean field equation is already in diagonal form with the Riemann invariant \bar{u} associated with the velocity V . The second Riemann invariant, q , depends on \bar{u} , a and is associated with the characteristic velocity c . It can be found by integrating $f d\bar{u} + (c - V)da$ (see, e.g., Ref. [5]). Another way of finding q is to look for a simple wave relation $a(\bar{u})$ of the subsystem (A10a) and (A10b).

The coupling function $f(a, \bar{u})$ is not always readily available, and its direct computation generally requires the determination of a singular, soliton limit in the full system of Whitham modulation equations for the dispersive hydrodynamics [25]. Below, we use a convenient change of variables proposed in Ref. [33] that enables one to circumvent explicit determination of the coupling function f in the derivation of the Riemann invariant q , utilizing only the known linear dispersion relation $\omega(k, \bar{u})$ and the soliton amplitude-speed relation $c(a, \bar{u})$.

Following Ref. [33], we introduce a conjugate (soliton) wavenumber $\tilde{k} = \tilde{K}(a, \bar{u})$, implicitly determined via the soliton amplitude-speed relation

$$c(a, \bar{u}) = \tilde{\omega}(\tilde{k}, \bar{u})/\tilde{k}, \quad (\text{A12})$$

where $\tilde{\omega}(\tilde{k}, \bar{u}) = -i\omega(i\tilde{k}, \bar{u})$ is the conjugate dispersion, whose phase velocity coincides with the speed of a soliton. The conjugate dispersion relation is realized by linearizing the governing dispersive hydrodynamic equation, Eq. (1), with respect to the soliton solution in the far-field. Very often, one can explicitly determine the soliton amplitude-speed relation $c(a, \bar{u})$ hence also the change of variables $\tilde{k} = \tilde{K}(a, \bar{u})$ via Eq. (A12).

As a simple example, for the KdV equation we have $\omega = k\bar{u} - k^3$, $c(a, \bar{u}) = \bar{u} + a/3$, therefore $\tilde{k}^2 = a/3$.

For the conduit equation, the dispersion and soliton amplitude-speed relations are [13]

$$\omega(k, \bar{u}) = \frac{2\bar{u}k}{1 + \bar{u}k^2}, \quad (\text{A13})$$

$$c_s(a, \bar{u}) = \frac{\bar{u}}{a^2} \{ (a + \bar{u})^2 [2 \ln(1 + a/\bar{u}) - 1] + \bar{u}^2 \}.$$

The conjugate wavenumber transformation (A12) then yields $\tilde{k}^2 = 1/\bar{u} - 2/c_s(a, \bar{u})$.

In the variables (\tilde{k}, \bar{u}) , simple wave solutions of Eqs. (A10a) and (A10b) satisfy the ordinary differential equation (ODE) [33]

$$\frac{d\tilde{k}}{d\bar{u}} = \frac{\tilde{\omega}_{\bar{u}}}{V(\bar{u}) - \tilde{\omega}_{\tilde{k}}}. \quad (\text{A14})$$

For the KdV equation, the ODE (A14) is readily integrated to yield $2\bar{u} + 3\tilde{k}^2 = q$, where q is a constant.

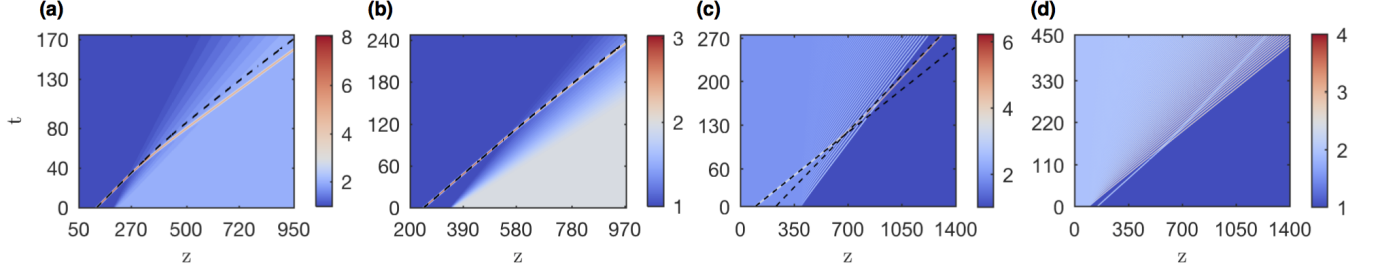


FIG. 5. Numerical simulations of the conduit equation (contours) and corresponding predicted soliton trajectories (dashed curves). a) Soliton-RW transmission for $a_- = 7$, $\bar{u}_- = 1$, and $\bar{u}_+ = 2$. The dashed curve is the integration of Eq. (A11). b) Soliton-RW trapping for $a_- = 2$, $\bar{u}_- = 1$, and $\bar{u}_+ = 2$. The dashed curve is the integration of Eq. (A11). c) Soliton-DSW transmission for $a_- = 2$, $\bar{u}_- = 2$, and $\bar{u}_+ = 1$. The two dashed curves correspond to the predicted soliton trajectory pre and post DSW interaction. The post interaction trajectory is determined by the adiabatic invariants $q(a, \bar{u})$ and $r(a, \bar{u})$. The difference between the z intercepts of these lines is the soliton-DSW phase shift. d) Soliton-DSW trapping for $a_+ = 1.5$, $\bar{u}_- = 2$, and $\bar{u}_+ = 1$.

For the conduit equation, integration of (A14) gives an implicit determination of $\tilde{k}(\bar{u})$

$$\frac{\bar{u}(2 - \bar{u}\tilde{k}^2)}{(\bar{u}\tilde{k}^2 - 1)^2} = q, \quad (\text{A15})$$

where q , again, is a constant of integration.

Generally, $q = q(a, \bar{u})$ is constant along the characteristic $dx/dt = C(q, \bar{u})$, where $C(q(a, \bar{u}), \bar{u}) \equiv c(a, \bar{u})$, and so is a Riemann invariant satisfying Eq. (A11b). For the KdV equation, we find $q = a + 2\bar{u}$ and $C = (q + \bar{u})/3$. For the conduit equation, we obtain $q(a, \bar{u}) = c(a, \bar{u})[c(a, \bar{u}) + 2\bar{u}]/\bar{u}$ and $C(q, \bar{u}) = -\bar{u} + \sqrt{\bar{u}(q + \bar{u})}$ (Eq. (5)).

Having determined two Riemann invariants, \bar{u} and $q(a, \bar{u})$, of the system (A10), the third Riemann invariant, labeled $r(q, \bar{u}, k)$ and also associated with the characteristic velocity $C(q, \bar{u})$, is readily found in the form $r = kp(q, \bar{u})$ where $p(q, \bar{u})$ is given by the general expression (4).

The constancy of q and r lead to the transmission conditions in Eq. (8). These conditions completely determine the soliton's trajectory post RW or DSW interaction. They also determine the conditions for soliton-hydrodynamic trapping. All four possible interaction types (soliton-RW, soliton-DSW trapping and transmission) are shown in the numerical simulations compared with theoretical predictions in Fig. 5.

Appendix B: Amplitude property of soliton transmission

Conduit soliton transmission through a RW has the following property. The amplitude of the transmitted soliton, a_+ , is always smaller than the amplitude of the incident soliton, $a_+ < a_-$. The same result readily follows for KdV soliton transmission using the first condition (8) and the expression $q = a + 2\bar{u}$ for the Riemann invariant derived in Sec. . We now derive the extension of

this result to the general dispersive hydrodynamic system Eq. (1), assuming $V'(u) > 0$.

In the mean field, simple wave approximation, the transmission of a soliton through a RW is determined by the conservation of the second Riemann invariant, $q(a, \bar{u})$, of the solitonic hydrodynamic system (A10) (see the first condition in Eq. (8)). We are interested in the sign of the derivative a_x in the course of soliton transmission. Expressing $a(q, \bar{u})$, we obtain $a_x = a_{\bar{u}}\bar{u}_x$ (since q is constant). Now, using Eq. (7), we have $\bar{u}_x = 1/(tV'(x/t)) > 0$. Next, $a_{\bar{u}} = -q_{\bar{u}}/q_a$. Hence, $\text{sgn } a_x = -\text{sgn}(q_{\bar{u}} q_a)$ and therefore, $\text{sgn}[a_+ - a_-] = -\text{sgn}[q_{\bar{u}} q_a]$ assuming $q_{\bar{u}} \neq 0$, $q_a \neq 0$. Say, for KdV $q = a + 2\bar{u}$ so $\text{sgn}[a_+ - a_-] = -1$ as already observed. By hydrodynamic reciprocity, the amplitude change for soliton-DSW transmission is opposite to that of soliton-RW transmission.

In a similar manner, the acceleration or deceleration of soliton-RW transmission can be determined by the positivity or negativity of C_x . By a similar argument, $\text{sgn}[C_x] = \text{sgn}[C_{\bar{u}}]$. For KdV, $C_{\bar{u}} = 1/3$, and for the conduit equation, $C_{\bar{u}} = c^2/[2\bar{u}(c + \bar{u})] > 0$, so a transmitted soliton in both cases is accelerated by the RW. By hydrodynamic reciprocity, a soliton is decelerated by a DSW.

Appendix C: Fluid Conduit Experimental Details

The experimental setup is similar to that described in [13] and consists of a square acrylic column with dimensions $5 \times 5 \times 183 \text{ cm}^3$. The column is filled with glycerol, a highly viscous, transparent, exterior fluid. A nozzle installed at the base of the column allows for the injection of the interior fluid. To eliminate surface tension effects, the interior fluid is a miscible solution of glycerol, water, and black food coloring. As a result, the interior fluid has both lower density and viscosity than

the exterior fluid. The properties of the interior and exterior fluids are dynamic viscosity $\mu^{(i)} = 51 \pm 1$ cP, $\mu^{(e)} = 1200 \pm 20$ cP and density $\rho^{(i)} = 1.2286 \pm 0.0001$ g/cm³, and $\rho^{(e)} = 1.2587 \pm 0.0001$ g/cm³ with a superscript denoting interior/exterior.

Interior fluid is drawn from a reservoir and injected through the nozzle via a computer controlled high precision piston pump. By injecting at a constant rate, the buoyant interior fluid establishes a stable, vertically uniform fluid conduit. By varying the injection rate in a precise manner, conduit solitons, RWs, and DSWs can be reliably generated. For each trial, a volumetric flow rate profile $Q(t)$ is generated based on these fluid properties that results in a long box followed by a soliton of chosen amplitude. The smaller conduit diameter is set by the background flow rate $Q = 0.25$ mL/min. The maximum flow rate for the long box is $Q = 0.7656$ mL/min. These two flow rates correspond to a nondimensional jump in cross-sectional area from 1 to 1.75 that defines \bar{u}_{\pm} . The box is sufficiently long that the trailing edge acts as a RW and leading edge acts as a DSW at the time of their respective interactions with the soliton.

The cross-sectional area of the fluid conduit corresponds to the dispersive hydrodynamic medium of interest. Data acquisition of \bar{u}_{\pm} and a_{\pm} is performed using three high resolution cameras, two equipped with macro lenses and one with a zoom lens. The macro lens cameras are near the bottom and top of the conduit, and the zoom lens near the middle, for extracting precise conduit diameter and soliton amplitude information. The cameras take several high-resolution images of the soliton as it passes through their respective viewscreens, as well as pictures of the background conduit before and after the hydrodynamic structure has passed. Correction for the refractive index of glycerin is calibrated via images of a cylinder of known height and width dropped into the center of the apparatus before the experiment.

The camera images are processed in MATLAB to extract the conduit edges by taking a horizontal row of pixels and calculating the maximum and minimum derivatives for each row. As the background is white and the conduit is black, this finds the approximate boundary. The conduit's slight variability from vertical gets enhanced during image processing so we use a background subtraction method to extract the measured non-dimensional conduit area from the images reported in Figs. 2 and 4. Prior to inducing interfacial dynamics, we take ten images, extract non-dimensional edge data, average all the edges and subtract this from edges extracted for the trial. The data is then sent through a low-pass filter to reduce noise from the pixelation of the photograph and any impurities (such as bubbles) in the exterior fluid. After converting to area and rescaling the smaller background area to unity, we then determine the soliton amplitudes before and after tunneling. Calculations suggest that density variations of 1% in the exterior

fluid can lead to a 10% change in the background conduit diameter. We observe an increase in the conduit diameter for the top camera, relative to the bottom and middle cameras by 10.1%, which we attribute to density variation of the external fluid. Because the model assumes no density variation, we accommodate this discrepancy by scaling all amplitude measurements from the top camera by the factor $1.101^2 = 1.212$.

This work was supported by NSF CAREER DMS-1255422 (DVA, NAF, MAH), the NSF GRFP (MDM), NSF EXTREEMS-QED DMS-1407340 (DVA), and EP-SRC grant EP/R00515X/1 (GAE). GAE and MAH gratefully acknowledge the London Mathematical Society for supporting a Research in Pairs visit.

* hoefer@colorado.edu

- [1] L. D. Landau and E. Lifshitz, *Fluid Mechanics*, 2nd ed. (Butterworth-Heinemann, 1987).
- [2] I. Carusotto and C. Ciuti, *Rev. Mod. Phys.* **85**, 299 (2013).
- [3] E. Fradkin, *Field Theories of Condensed Matter Physics*, 2nd ed. (Cambridge University Press, Cambridge, UK, 2013).
- [4] R. E. Wyatt and C. J. Trahan, *Quantum dynamics with trajectories: introduction to quantum hydrodynamics*, Interdisciplinary applied mathematics v. 28 (Springer, New York, 2005).
- [5] G. B. Whitham, *Linear and nonlinear waves* (Wiley, New York, 1974).
- [6] G. A. El and M. A. Hoefer, *Physica D* **333**, 11 (2016).
- [7] A. V. Gurevich and L. P. Pitaevskii, *Sov. Phys. JETP* **38**, 291 (1974), translation from Russian of A. V. Gurevich and L. P. Pitaevskii, *Zh. Eksp. Teor. Fiz.* **65**, 590-604 (August 1973).
- [8] M. A. Hoefer, M. J. Ablowitz, I. Coddington, E. A. Cornell, P. Engels, and V. Schweikhard, *Phys. Rev. A* **74**, 023623 (2006).
- [9] Y. C. Mo, R. A. Kishek, D. Feldman, I. Haber, B. Beaudoin, P. G. O'Shea, and J. C. T. Thangaraj, *Phys. Rev. Lett.* **110**, 084802 (2013).
- [10] W. Wan, S. Jia, and J. W. Fleischer, *Nat. Phys.* **3**, 46 (2007).
- [11] G. Xu, M. Conforti, A. Kudlinski, A. Mussot, and S. Trillo, *Phys. Rev. Lett.* **118**, 254101 (2017).
- [12] S. Trillo, M. Klein, G. Clauss, and M. Onorato, *Physica D* **333**, 276 (2016).
- [13] M. D. Maiden, N. K. Lowman, D. V. Anderson, M. E. Schubert, and M. A. Hoefer, *Phys. Rev. Lett.* **116**, 174501 (2016).
- [14] P. A. Praveen Janantha, P. Sprenger, M. Hoefer, and M. Wu, *Phys. Rev. Lett.* **119**, 024101 (2017).
- [15] N. J. Zabusky and M. D. Kruskal, *Phys. Rev. Lett.* **15**, 240 (1965).
- [16] P. G. Drazin and R. S. Johnson, *Solitons: an introduction* (Cambridge University Press, Cambridge, UK, 1989).
- [17] M. Remoissenet, *Waves called solitons: concepts and experiments*, 3rd ed. (Springer, New York, 2013).
- [18] N. K. Lowman and M. A. Hoefer, *Phys. Rev. E* **88**,

- 023016 (2013).
- [19] P. Olson and U. Christensen, *J. Geophys. Res.* **91**, 6367 (1986).
 - [20] D. R. Scott, D. J. Stevenson, and J. A. Whitehead, *Nature* **319**, 759 (1986).
 - [21] N. K. Lowman, M. A. Hoefer, and G. A. El, *J. Fluid Mech.* **750**, 372 (2014).
 - [22] B. Selvam, L. Talon, L. Lesshafft, and E. Meiburg, *J. Fluid Mech.* **618**, 323 (2009).
 - [23] G. El, M. Hoefer, and M. Shearer, *SIAM Rev.* **59**, 3 (2017).
 - [24] R. Grimshaw, *Proc. R. Soc. Lond. A* **368**, 359 (1979).
 - [25] A. V. Gurevich, A. L. Krylov, and G. A. El, *Sov. Phys. JETP* **71**, 899 (1990).
 - [26] G. A. El, R. H. J. Grimshaw, and A. M. Kamchatnov, *J. Fluid Mech.* **585**, 213 (2007).
 - [27] G. A. El, R. H. J. Grimshaw, and W. K. Tiong, *J. Fluid Mech.* **709**, 371 (2012).
 - [28] R. Grimshaw and C. Yuan, *Physica D* **333**, 200 (2016).
 - [29] R. Grimshaw and C. Yuan, *Nat. Hazards* **84**, S493 (2016).
 - [30] Y. S. Kivshar and B. A. Malomed, *Rev. Mod. Phys.* **61**, 763 (1989).
 - [31] N. K. Lowman and M. A. Hoefer, *J. Fluid Mech.* **718**, 524 (2013).
 - [32] P. Sprenger, M. A. Hoefer, and G. A. El, preprint arXiv:1711.05239 (2018).
 - [33] G. A. El, *Chaos* **15**, 037103 (2005).